CFD modeling of water spray interaction with dense gas clouds

Robert N. Meroney [a],
[a]*Wind Engineering Software, Fort Collins, CO,USA, Robert.Meroney@ColoState.Edu*

1 INTRODUCTION

Water spray curtains can provide an effective and rapid dilution mechanism for low lying dense clouds. Frequently such clouds are released as a result of a chemical manufacturing, storage or gas transportation accident. Gases of concern include cold liquefied natural gas (LNG), refrigerated rocket propellants or oxidants, agricultural chemicals (ammonia), gaseous fuels (propane) or other high-molecular weight gases (fluorinated hydrocarbons). Since for most atmospheric conditions the dense gases will remain negatively buoyant for significant time intervals, a ground-level hazard may exist due to gas flammability or toxicity.

Extensive field and laboratory tests have been performed to determine how well water curtains can mitigate actual spill conditions (Blewitt et al, 1987; Heskestad et al., 1983; Meroney et al., 1984; Moodie et al., 1981). Numerical methods are often proposed to provide system design or timely response information (Meroney, 1984a, 1984b, 1985, 1989, 1991; Meroney and Neff, 1985). Most of these models reduce mathematical and computational complexity by integrating the equations of motion over volumes, sections or depths which provides computational speed but often sacrifices mixing detail and typically presume the use of empirical entrainment relationships. In this paper computational fluid dynamics (CFD) has been used to reproduce the water-spray/cold carbon dioxide releases performed by Moodie et al., 1981. Parallel wind tunnel experiments were described by Heskestad et al, 1983, and specific comparisons to box and slab models were presented by Meroney et al., 1983, and Meroney and Neff, 1985. Thus, there is an opportunity to provide side-by-side comparisons of field, wind tunnel, box, slab and CFD modeling methods.

1.1 *The HSE Experimental Configuration*

A field test series was performed by the Health and Safety Executive, U.K., in 1981 using cold CO_2 vapor (-79° C) at an estimated spill rate of 1.1 kg sec^{-1} from a point source (Moodie et al., 1981). Although a number of tests were performed with and without water sprays activated, initially only two of these were chosen for physical modeling, Trials HSE 41 and HSE 46, because of the availability of model size nozzles, practical scaling ratios, and apparent quality of the data (Meroney et al., 1984). Subsequently it was determined that during HSE 41 additional field features such as source icing, upwind storage tanks, wind meandering, and wind speed variations affected the plume. Communication with HSE personnel revealed that the wind instrumentation was in the wake of other test equipment during the test. Thus, the model data for only Trial HSE 46 will be considered here.

During HSE field Trial 46 the wind speeds at a height of 1.25 m were reported to average 1.7 ± 0.5 m sec^{-1} while wind direction veered ± 5°. Surface drag and roughness were estimated as u^*/u_{ref} = 0.05 and z_o = 6.5 mm, respectively (equivalent to a power law coefficient, n = 0.178). During both wind tunnel and numerical calculations the cold CO_2 was replaced by an isothermal dense simulant with an equivalent specific gravity, SG, of 2.35. Eight ground level samplers (P' to W') and 12 elevated samplers above points T', V' and W' were positioned downwind of the field source as shown in Figure 1. Additional sampling points, A' to O', were inserted during wind tunnel and numerical simulations. Dense simulant gases were released to produce a Froude number scaled volume flow equivalent to a CO_2 spill rate of 1.1 kg sec^{-1}. Twenty water spray

nozzles pointed vertically down and spaced 1.66 m apart at a height of 3 m were position approximately 5 m downwind of the source gas location at a ~13° angle to the wind as noted in Figure 1

1.2 *Wind Tunnel Simulation Configuration*

The HSE Trials 41 and 46 were modeled at a scale ratio of 1:28.9 in the Meteorological Wind Tunnel at Colorado State University. This atmospheric boundary-layer wind tunnel has a test section 3.66 m wide, 2.28 m tall, and 17.0 m long. Vortex generators and a wall trip at the test section entrance produced a boundary layer about 1 m deep at the experiment location, 9.2 m downwind of the entrance. The modeled velocity profile was found to match the field measurements closely (Meroney et al., 1984). During modeled HSE 46 twenty Model 19577604 Sprayco Inc. spray nozzles with a nozzle diameter of 0.46 mm and angle of 38° were placed 5.66 cm (1.66 m) apart at a height of 10.4 cm (3 m) pointing vertically downward as in the field. Spray nozzle physics and nozzle selection are discussed by Heskestad et al. (1983). The source gas flowrate used to simulate the cold CO_2 was a mixture of CO_2, CCl_2Fl_2, and C_2H_6 to produce an equivalent specific gravity value (i.e. 2.35) of the cold CO_2 field plume was 87 ccs. Concentrations were measured with a flame-ionization detector in a gas chromatograph using samples drawn above the model iso-kinetically. Concentrations were measured to less than 0.1% with an accuracy of ±5%.

1.3 *Integral Based Numerical Models*

Computational techniques for dense gas cloud dispersion generally fall into four categories depending on the simplicity of the models—box models (volume integrated), slab models (cross-section integrated) shallow layer (depth integrated), and full 3-d field models (K or advanced turbulence models).

Box and slab models require the stipulation of boundary entrainment rates which are normally prescribed in terms of local relative cloud velocities (U and Re) frontal velocities (u_g), boundary friction (u_*) stratification (Ri_*, Gr) and for cold gases the temperature potential (T^*) or convective velocity (w_*) such that the entrainment velocity, $w_e = f(u_g, u_*, w_*, Ri_*, Re)$. (Meroney, 1983, 1984a, 1984b, 1985) Empirical coefficients in these solution procedures are assigned based on comparison with field or model experiments; hence, the results are often dependent on the data set used to calibrate the calculation scheme. Additional empirical modifications to such entrainment coefficients are made to account for the effect of vapor barrier fences and/or water-spray systems (Meroney 1989, 1991; Meroney and Neff, 1985).

2 NUMERICAL PREDICTION OF WATER SPRAYS AND DENSE CLOUD BEHAVIOR

Finally, solution of the full 3-dimensional equations of motion, energy, and species concentration are possible using a CFD code which solves the full set of partial differential equations in space and time. One no longer presumes similarity in vertical profiles in plume properties (velocity, concentration, species concentration, etc.), entrainment velocities and dilution are not specified but calculated as a result of the joint effects of advection and turbulence. Specification of appropriate inflow conditions, surface boundary conditions, material properties and an appropriate turbulence model become crucial. The turbulence models should include components which adjust for the damping effects of thermal or density stratification on turbulent generation and dissipation. CFD modeling of water spray barriers have previously been performed by Gant (2006) and Mawhinney and Trelles (2007) using the CFX and FDS codes respectively.

In this case I chose to use the public domain Fire Dynamic Simulator (FDS) software developed by the U.S. National Institute of Standards and Technology (McGrattan et al. 2009a, 2009b). This software uses a particularly fast solver on hexagonal cell grids, but it permits easy inclusion of water-spray nozzles and specification of inlet boundary-layer profiles, dense-gas sources, and

various detectors. Solutions were obtained on a domain 100 m long, 100 m wide and 10 m tall. Meshes were graded in the vertical from 0.1 m to 0.7 m, horizontal cells were 0.5 m x 0.5 m for a total cell count of 600,000. The model uses the Smagorinsky version of the large-eddy-simulation (LES) turbulence model with a low-Mach number version of the equations of motion (hence, they will not calculate acoustic waves).

The NIST model assumes a spray consists of a sampled set of spherical droplets whose size distribution is specified by a combination of log-normal and Rosin-Rammler distributions. Discharge velocity is computed from the specified mass flow rate. Every droplet from a given sprinkler or nozzle is not tracked, instead a sampled set of droplets is tracked which use weighting constants to characterize the mass, momentum and energy transported by the sample particle. The individual droplets are tracked by Lagrangian equations of motion which include drag forces induced by relative motions of the droplet and gas surroundings. In turn the momentum transferred from the droplets to the gas is obtained by summing the force transferred from each sample droplet in a grid cell and dividing by the cell volume (McGrattan et al., 2009b).

An inlet atmospheric boundary layer profile with a power-law coefficient of 0.178 was specified such that U = 1.7 m/s at a height of 1.25 m. The dense gas source was located 50 m downwind from the entrance. Sampling locations were specified at all field and wind tunnel measurement locations. The dense gas was simulated by a SG=2.35 tracer flowing in at 0.39 m^3 sec^{-1} and the twenty water-spray nozzles were specified to spray downward from a height of 3m at a rate of of 33.7 liters min^{-1}. (Additional runs were also calculated for SG=1.52, which typifies the density of CO_2 due to molecular weight alone.) The water droplets (density = 1000 kg m^{-3}) were injected through a 14 mm nozzle at a rate of 5000 droplets/second at a constant size of 500 μm at each nozzle. The droplets were removed on contact with the ground.

2.1 *No spray configuration*

The numerical system without a water-spray curtain was first run to produce a base case situation. Calculations were performed out to 240 seconds, but the flow was essentially stationary over the domain after ~100 sec. Velocity profiles and concentration patterns were followed along cross-wind slices and along the ground, and concentration time series were recorded at all samplers A' to W'.

2.2 *Water spray configuration*

The same conditions were examined but with the 20 water-spray nozzles active at all times.

3 DISCUSSION OF RESULTS

All field, wind tunnel and FDS results are compared in a logarithmic scatter plot in Figure 2. Notice that all no-spray measurements compare quite closely with the field measurements producing a regression coefficient, r, of 0.962 for field to wind tunnel and 0.881 for field to FDS data. Spray measurements agree well with coefficients of 0.990 and 0.977 for the field to wind tunnel and FDS data, respectively, but with an off-diagonal bias.

Figure 3 displays the resultant concentrations versus the radial distance from the source locations A to O noted in Figure 1. Spray and no-spray concentrations both decay at a power law rate of about -0.5, but after the spray line the concentrations are diminished by a factor of about 4 to 5. Figure 4 considers the lateral distribution of concentrations at field probe positions A to O. Although the wind tunnel and FDS predictions both display the expected cross-flow profiles and the reductions associated with water spray dilution, the wind tunnel data are deflected toward the south and at samplers F and G , and the FDS SG= 2.5 cloud seems to have passed between the spray nozzles resulting in higher concentrations.

Figure 5 examines the predicted Percent Dilution by the wind tunnel and FDS models where PD = 100 ($C_{\text{no water spray}} - C_{\text{water spray}}$)/$C_{\text{no water spray}}$. Moore and Rees (1981) suggested comparison using a forced diffusion ratio, FD = ($C\%_{\text{wo spray}} * U_{\text{w spray}}$)/($C\%_{\text{w spray}} * U_{\text{wo spray}}$) displayed in Figure 6. The FD values between field and wind tunnel measurements and field and FDS predictions correlated with one another with regression coefficients of 0.910 and 0.620, respectively.

Figures 7 to Figure 11 display horizontal and vertical concentration contours for no-spray and spray conditions at a time, t = 300 sec. Notice how the surface concentrations diminish abruptly at the water spray line and the cloud depth increases downstream of the nozzles. Figure 11 shows how the spray modifies the velocity contours in the wake of the nozzles and spray region, and how tracer particles emitted from the CO_2 source are deflected laterally around the spray curtain.

4 CONCLUSIONS

Both the wind tunnel and the CFD methods tended to over predict the dilution ability of the water spray system. The wind tunnel model tended to over predict no-spray values and under predict spray values, resulting in over prediction of FD. The FDS model tended to predict no-spray values about right, but produced wide scatter in the spray conditions. This could be due to reduced plume width downstream of the water curtain or just be uncertainties in the field measurements. It is also likely due to the dilution patterns produced by nozzle placement.

5 REFERENCES

Blewitt, D.N., Yohn, J.F., Koopman, R.P., Brown, T.C., and Hague, W.J. (1987), Effectiveness of water sprays on mitigating anhydrous hydrofluoric acid releases, *Proc. Int. Conf. on Vapor Cloud Modeling*, CCPS, Cambridge, MA, 2-4 November, 155-180.

Gant, S.E., (2006), CFD Modelling of Water Spray Barriers, Health and Safety Laboratory, UK, Report HSL/2006/79, 35 pp.

Heskestad, G., Meroney, R.N., Kothari, K.M. and Neff, D.E. (1983), Effectiveness of water spray curtains in dispersing LNG vapor clouds, *AGA Transmission Conference*, Seattle, Washington, 2-4 May 1983, 41 pp.

Mawhinney, J.R. and Trelles, J. (2007), Computational fluid dynamics modeling of water mist systems on large HGV fires in tunnels, Journee dEtude Technique: Brouillard dEau – Quoi de Neuf? At Pole Europeen de Securite CNPP- Vernon, France, November 22, 36 pp.

McGrattan, K., Hostikka, S., and Floyd, J. (2009a), Fire Dynamics Simulation (Version 5) User's Guide, U.S. Dept. of Commerce, National Institute of Standards and Technology, *NIST Special Publication 1019-5*, 224 pp.

McGrattan, K., Hostikka, S., Floyd, J., Baum, H., Rehm, R., Mell, W. and McDermott, R. (2009b) Fire Dynamics Simulator (Version 5) Technical Reference Guide, Volume 1: Mathematical Model, U.S. Dept. of Commerce, National Institute of Standards and Technology, *NIST Special Publication 1018-5*, 110 pp.

Meroney, R.N. (1984a), Transient characteristics of dense gas dispersion. Part I: A depth-averaged numerical model, *J. of Hazardous Materials*, Vol. 9, 139-157.

Meroney, R.N. (1984b), Transient characteristics of dense gas dispersion. Part II: Numerical experiments on dense cloud physics, *J. Hazardous Materials*, Vol. 9, 159-170.

Meroney, R.N. (1985), A time-dependent, quasi-three dimensional depth-integrated numerical model to calculate surface heat transfer and entrainment to cold fluid intrusions, *Int. Symp. On Defined Plane Modeling and Turbulence Measurements*, 16-18 September, 1985, Iowa City, Iowa, 12 pp.

Meroney, R.N. (1989), Dilution of hazardous gas cloud concentrations using vapor barriers and water spray curtains, *Recent Advances in Wind Engineering*, editor T.F.Sun, (Proceedings of *2nd Asia-Pacific Symposium on Wind Engineering*, Beijing, China 26-29 June 1989,) International Academic Publishers, Pergamon Press, Beijing, 1989, Vol. 2, pp. 930-936

Meroney, R.N. (1991), Numerical simulation of the mitigation of HF cloud concentrations by means of vapor barriers and water spray curtains, *AIChE Int. Conf. and Workshop on Modeling and Mitigating the Consequences of Accidental Releases of Hazardous Materials*, New Orleans, Louisiana, 21-24 May 1991, 12 pp.

Meroney, R.N., Neff, D.E., and Heskestad, G. (1984), Wind-tunnel simulation of field dispersion tests (By the U.K. Health and Safety Executive) of water-spray curtains, *Boundary-Layer Meteorology*, Vo. 28, 107-119.

Meroney, R.N. and Neff, D.E. (1985), Numerical modeling of water spray barriers for dispersing dense gases, *Boundary Layer Meteorology*, Vol. 31, 233-247.

Moodie, K., Taylor, G., and Beckett, H. (1981), Water spray barrier trials: 181, Test Parameters and Concentration Data for Trials 35-48, *Health and Safety Executive Report FM/15/81/3*, 60 pp.

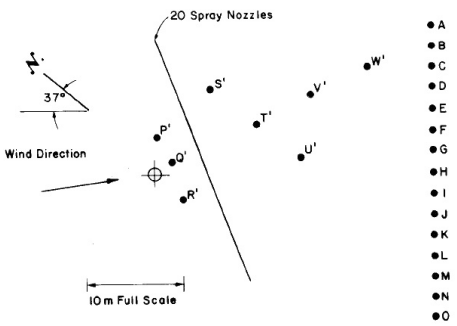

Figure 1: Plan view of HSE Trial Number 46.

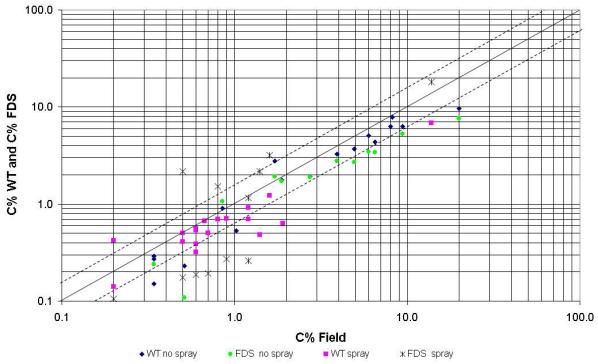

Figure 2: Logarithmic scatter diagram comparing HSE field, wind tunnel and FDS concentrations.

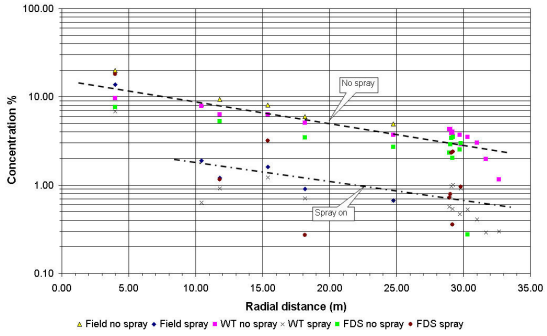

Figure 3: Concentrations versus radial distance from the source location.

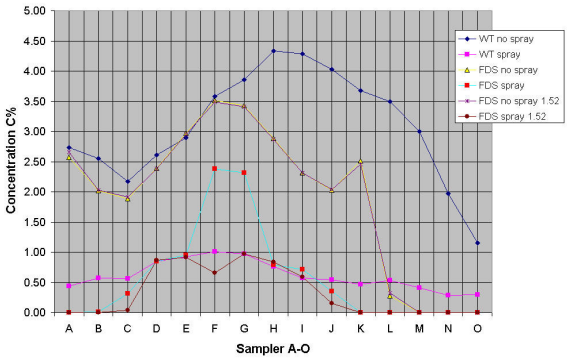

Figure 4: Concentrations vs Probe Postion A to O found in wind tunnel and CFD models

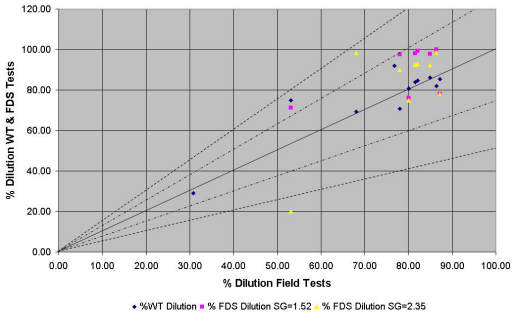

Figure 5: Percent dilution

$PD = 100\ (C_{\text{no water spray}} - C_{\text{water spray}})/C_{\text{no water spray}}$.

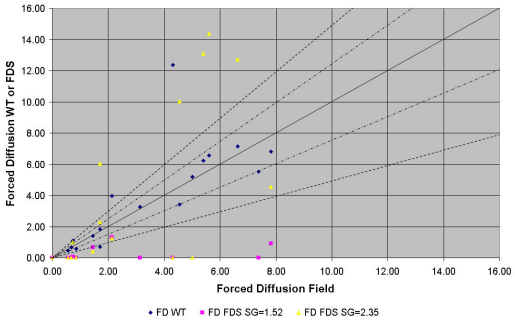

Figure 6: Forced diffusion

$FD = C_{\text{no water spray}} / C_{\text{water spray}}$

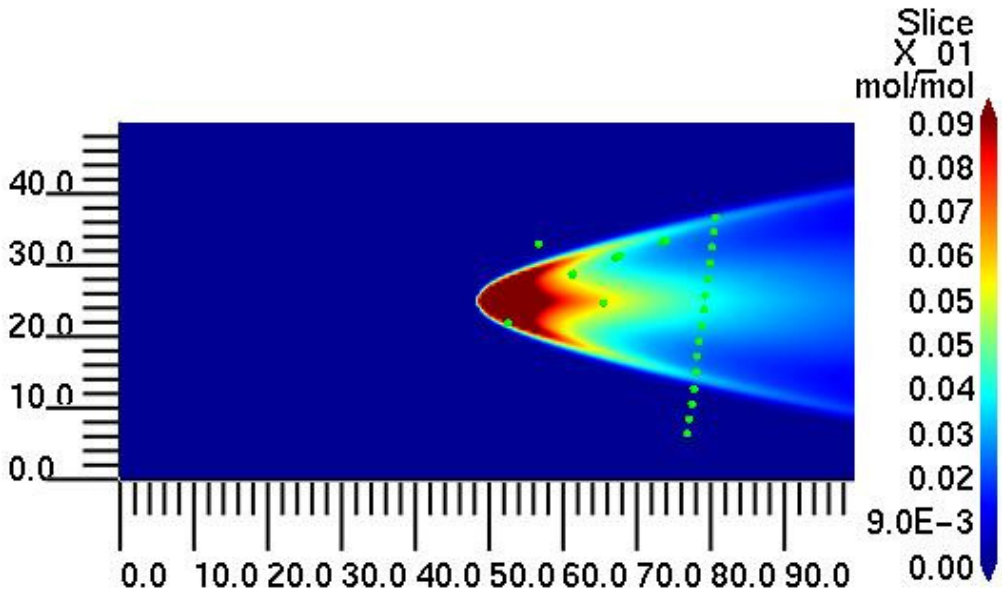

Figure 7: Concentration contours for no-spray condition at t = 300 sec.

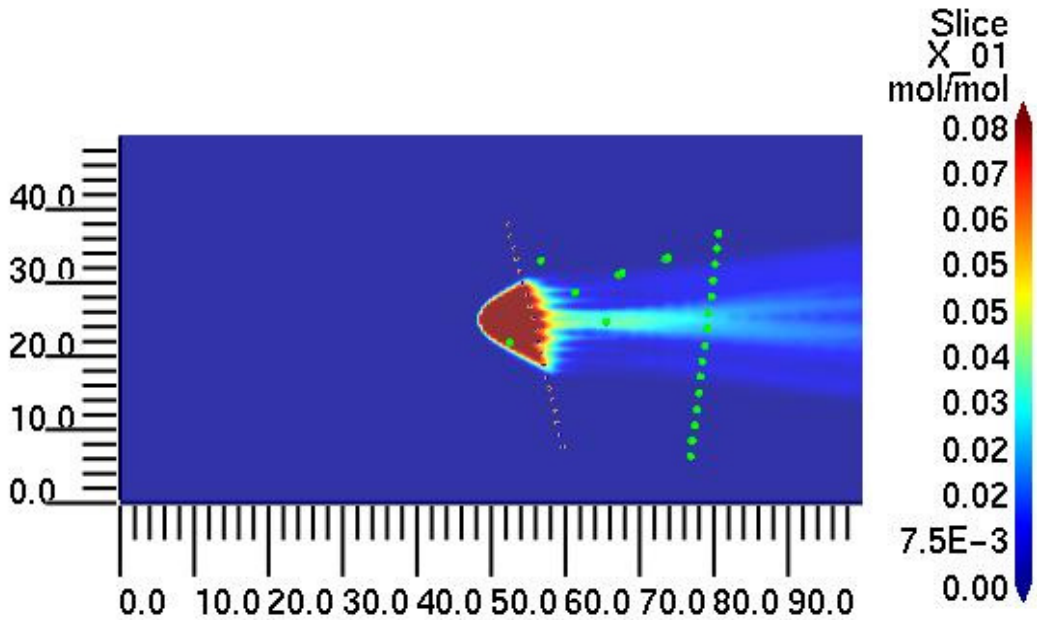

Figure 8: Concentration contours for spray condition at t = 300 sec.

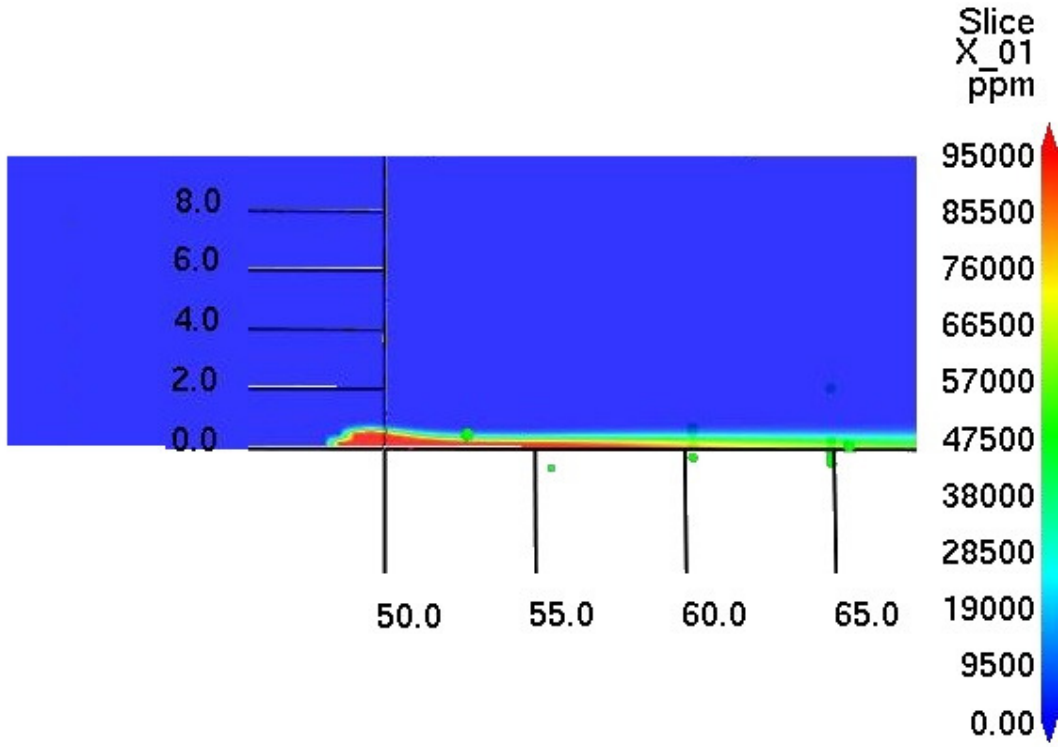

Figure 9: Concentration contours for no-spray condition at t = 300 sec. Y = 25 m cross section.

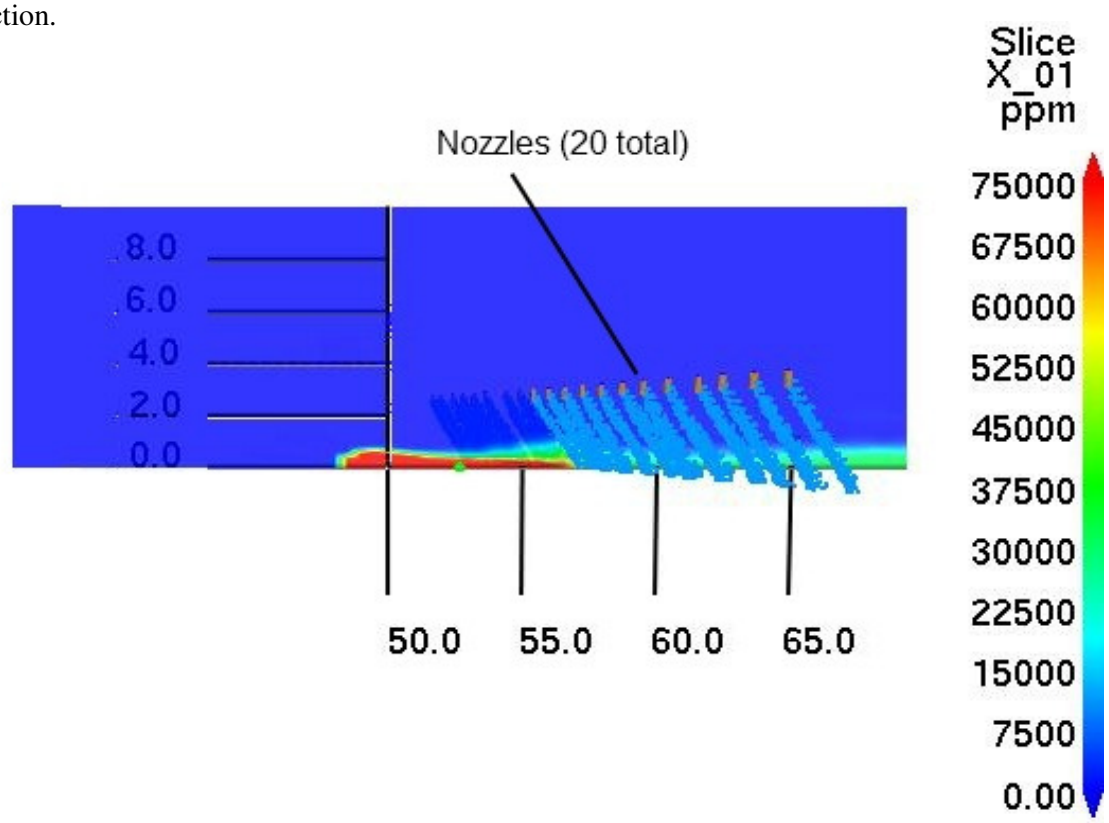

Figure 10: Concentration contours for spray condition at t= 300 sec. Y = 25 m cross section.

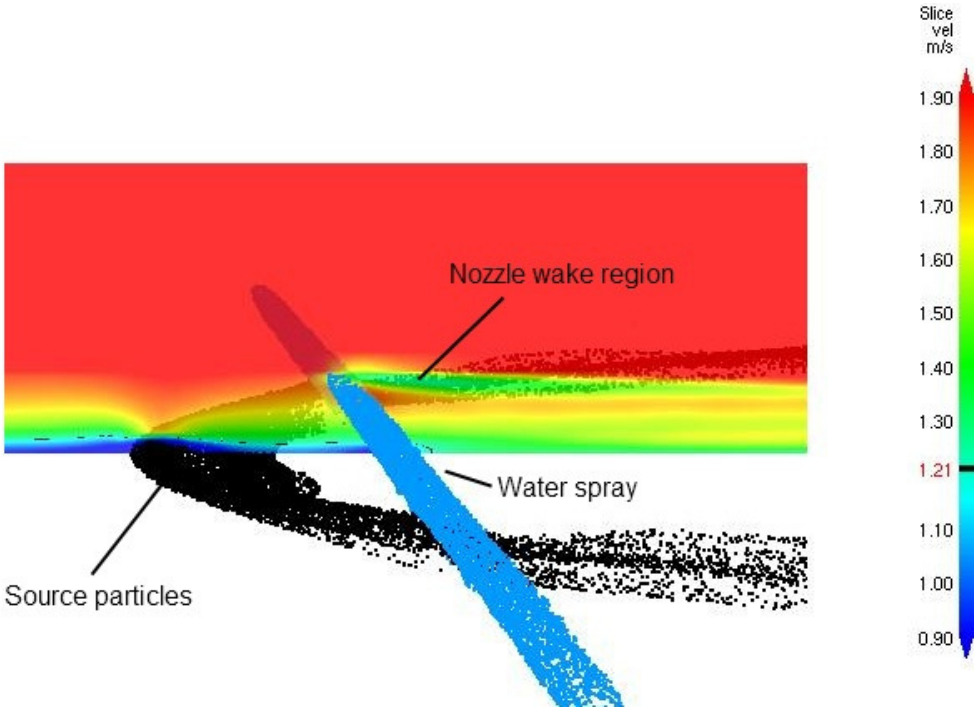

Figure 11: Velocity contours for spray condition at t = 300 sec. Y = 25 m cross section.